CHAPTER II

BACKGROUNDS AND LITERATURE REVIEW

2.1 Photocatalytic reaction

The photocatalytic process has been employed in heterogeneous photochemical advance oxidation processes (AOPs) for the eradication of contaminants in the air and wastewater. This process is used due to its aptitude for oxidizing many kinds of organic substances and reducing the charge of metal ions, changing them to non-toxic forms (Dionysiou et al., 1999). The term of photocatalysis is expounded as a reaction which is accelerated by photons from the light source and a catalyst (Hermann, 1999).

The principle role of photocatalysis is to adsorb a catalyst on a carrier and irradiate the system. When catalysts are exposed to the appropriate wavelength, electrons in the low energy valence band (VB) will absorb the photon's energy, become excited and move into the high energy conduction band (CB) (EPA, 1998). The result of this electron excitation is a hole or positive charge in the valence band (h^+_{VB}) and an electron in the conduction band (e^-_{CB}) as shown in Figure 2.1. So, at the conduction band an excited electron can react with the metal ions that are so-called the photocatalytic reduction. While, at the valence band the hole can receive an electron from the organic substances or some electron donors that is called the photocatalytic oxidation.
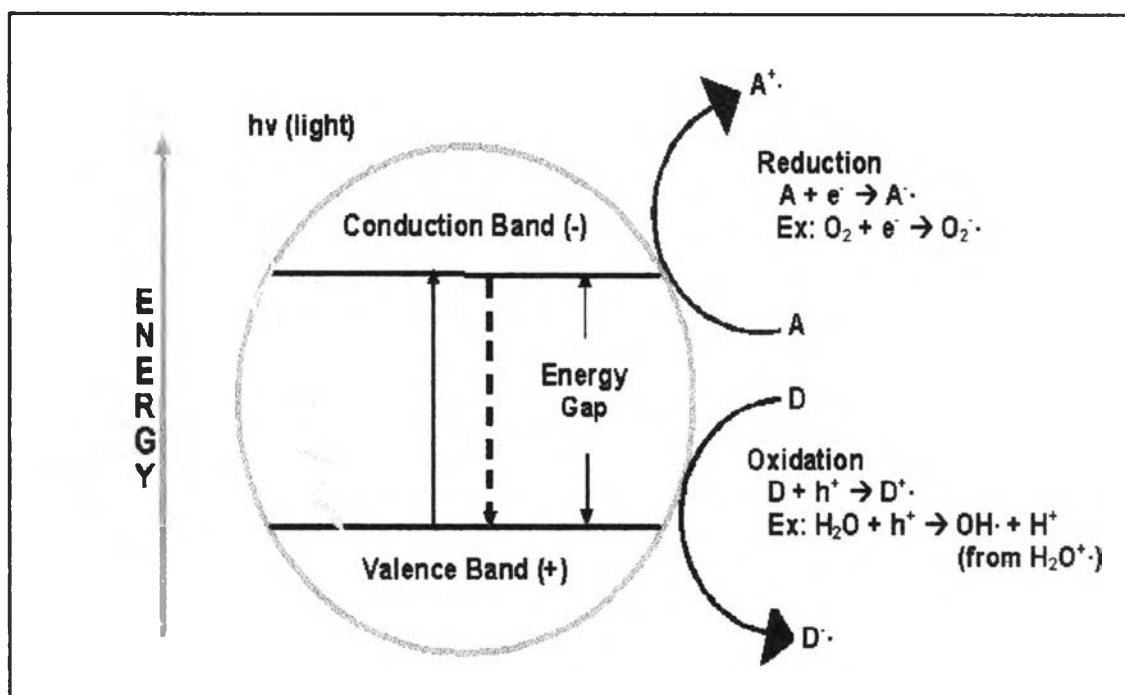
Figure 2.1 the scheme of photocatalysis

(http://dev.nsta.org/evwebs/ 1952/photocatalysis.htm: Available: Oct 25, 2005)

However, the energy should be more than the band gap (Eg), which is the region between the valence band (VB) and the conduction band (CB) then electrons can exist. When trapping by electron donors such as water (H_2O) occurs, the products are h+ and OH* radicals. So, these electrons and hole pairs can react with the contaminants, which are adsorbed on the catalyst surface indicating to the intermediates during the mineralization. The equations are as follows:

$$h^+_{VB} + H_2O \longrightarrow H^+ + OH^{\bullet} \tag{Eq.1}$$

$$OH^{\bullet} + (RH)_{ad} \longrightarrow H^+ + R^{\bullet} \longrightarrow \longrightarrow (\text{Intermediates; Int})_{ad} \tag{Eq.2}$$

$$OH^{\bullet} + (Int)_{ad} \longrightarrow H^+ + (Int)_{ad}^{\bullet} \longrightarrow \longrightarrow \text{mineralization} \tag{Eq.3}$$

With regard to the conduction band, electron acceptors such as metal ions, can reduce the charge and change them into non-hazardous forms, as shown below:

$$e^-_{CB} + (M^+)_{ad} \longrightarrow (M^0)_{ad} \tag{Eq.4}$$

Hence, it is illustrated that the metal ions (Cd, Hg, Cu, and Pb) in the photocatalytic reduction can prevent the holes recombination, while the photocatalytic oxidation occurs. The prevention of the radicals will help to increase the efficiency in the reduction process. From this point of view, both reactions will occur together, and the application of this process can convert organic toxic substances and metal ions to be mineralized at the same time.

Hermann, 1999 explained that the basic fundamental principles described the influence of the main parameters that deal with kinetics (mass of the catalyst, wavelength, initial concentration, temperature and radiant flux). Heavy toxic metal ions (Hg $^{2+}$, Ag$^+$, noble metals) could be removed from wastewater by photodeposition on titania (TiO$_2$). Several water detoxification photocatalytic devices have already been commercialized.

Kajivichyanukul and Watcharenwong, 2005 found that the adsorption of chromium (VI) on a TiO$_2$ surface was monolayer, following the Langmuir adsorption isotherm. The optimum time to reach equilibrium during adsorption was 10 minutes. Moreover, the amount of adsorbed chromium (VI) was higher in acidic pH than in basic pH.

2.2 Titanium dioxide or Titania (TiO$_2$)

Some types of catalysts, which are present in the photocatalytic process (for example, TiO$_2$, ZnO, CdS and Fe$_2$O$_3$) can be used depending on the reaction.

Further, titanium dioxide/ UV systems have been developed for a variety of chemical species with much success (Legrini et al., 1993). To establish an available titanium dioxide/ UV system, the photocatalyst must be immobilized. Some options for the immobilization include both the integration of titanium dioxide within thin films, mesh structures, or ceramics in plug-flow reactors; and titanium dioxide covered supports, such as glass beads or tubes, and in fluidized bed reactors (Chang et al., 2000; Legrini et al., 1993; Hoffman et al., 1995).

Three crystalline configurations of titanium dioxide exist: anatase, rutile, and brookite (EPA, 1998). The rate of hydroxyl radical formation depends on the crystalline forms of titanium dioxide present (EPA, 1998). Of the three possible configurations of titanium dioxide, the anatase form has the highest level of photoconductivity with a band gap of 3.2 electron volts (EPA., 1998; Munter et al., 2001). Rutile is considered much less photoreactive than anatase (Bahnemann, 1999; Munter et al., 2001). Figure 2.2 indicated the structures of the anaatase and rutile phases with their properties due to their characteristics for photocatalysis. This is attributed to its more efficient recombination of the electron-hole pair and a smaller surface area in the rutile structure (Munter et al., 2001). One of researches has indicated that it may be an optimum combination of rutile and anatase crystals for photocatalysis (Ollis and Turchi, 1990). Degussa P25 is commercially accepted as a standard photocatalytic form of titanium dioxide (Bahnemann, 1999; Hoffman et al., 1995; Legrini et al., 1993). Some important properties corresponding to their structures were showed in Table 2.1.
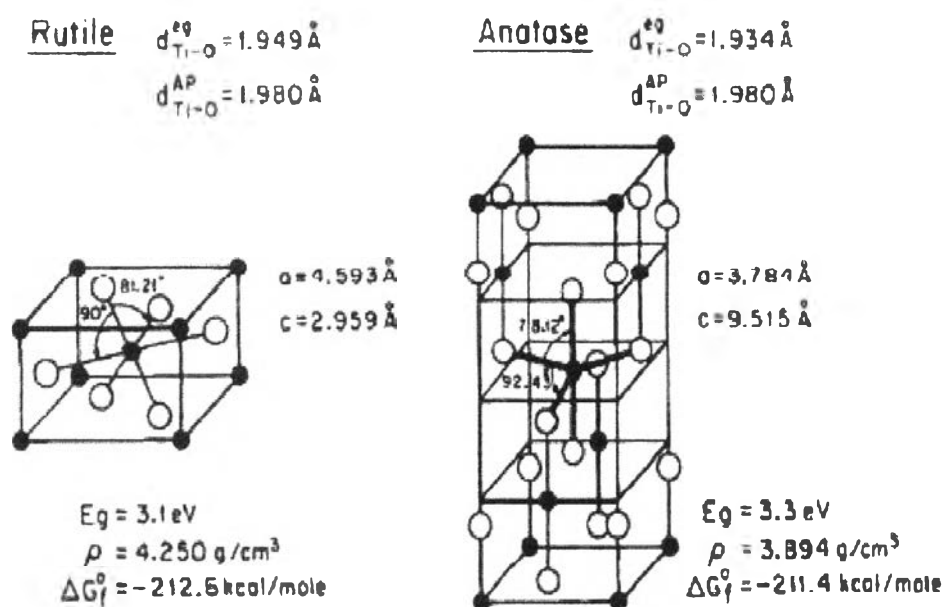
Rutile $d_{Ti-O}^{eq} = 1.949 Å$
          $d_{Ti-O}^{AP} = 1.980 Å$

Anatase $d_{Ti-O}^{eq} = 1.934 Å$
          $d_{Ti-O}^{AP} = 1.980 Å$

$a = 4.593 Å$
$c = 2.959 Å$

$a = 3.784 Å$
$c = 9.515 Å$

$Eg = 3.1 eV$
$\rho = 4.250 \, g/cm^3$
$\Delta G_f^0 = -212.6 \, kcal/mole$

$Eg = 3.3 eV$
$\rho = 3.894 \, g/cm^3$
$\Delta G_f^0 = -211.4 \, kcal/mole$

Figure 2.2   the structures of the rutile and anatase TiO$_2$ crystallite

(Linsebigler et al., 1995)

Table 2.1 The properties of the anatase and rutile phase

(Linsebigler et al., 1995; Fujishima et al., 1999; Litter, 1999)

Properties	Anatase	Rutile
Crystalline form	Orthorhombic	Orthorhombic
Band gab energy (eV)	3.200	3.030
Band gab wavelength (nm)	384	411
Hardness (Mohs)	5.5 – 6.0	6.0 – 7.0
Density (g/cm^3)	3.894	4.250
Gibbs free energy , ΔG_f° (kcal/mole)	-211.4	-212.6
Littice constant, a (A°)	3.784	4.593
Littice constant, c (A°)	9.515	2.959
Melting point	Changes to rutile at high temperature $\approx$ 800 °C	
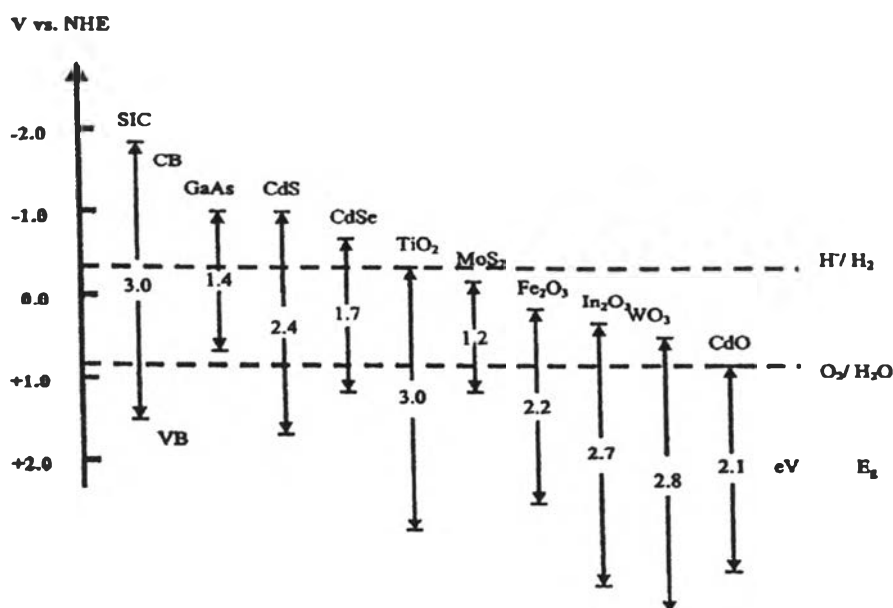
Figure 2.3 the band-gap energy of semiconductors

(http://www.ecodevice.co.jp/borders/Bandgap-E.gif: Available: Oct 25, 2005)

The key to semiconductor-induced reactions is a light source that will emit photons at the optimum wavelength for the excitation of the valence band electrons, an optimum that varies between semiconductors (EPA, 1998). Figure 2.3 showed the band gap energy which is important to note that titanium dioxide has a better band gap more than others. To excite titanium dioxide's valence band electrons, a light source must have a wavelength shorter than 387.5 nanometers to overcome the band-gap energy (EPA, 1998; Munter et al., 2001; Bahnemann, 1999). Medium-pressure, ultra-violet lamps provide the most effective source of photons for titanium dioxide systems, emitting wavelengths concentrated in the 200 to 400 nanometers range. Wavelengths shorter than 387.5 nanometers are emitted by the sun but in a much less concentrated and consistent manner, making the utilization of solar energy possible but much less advantageous than artificial sources (Legrini et al., 1993).

Negishi et al., 1995 prepared the transparent TiO_2 thin film photocatalyst and its photocatalytic activity. Transparent TiO_2 thin films were prepared on glass substrates via the sol-gel method from tetraisopropyl titanium ethanol solution containing polyethylene glycol and diethylene glycol. The transparency of these thin films was 80% in the visible. The photocatalytic activity of the TiO_2 thin films was studied using the deposition of acetaldehyde in the gas phase. The quantum yield with those films was similar to most of the photoactive commercial TiO_2 powders, such as Degussa P25. The key factor of this preparation was the addition of the organic/polymer components into the starting solution under low humidity conditions.

Shang et al., 2003 studied the structure and photocatalytic characteristics of having TiO_2 film photocatalyst coated on a stainless steel webnet by the sol-gel method. The stainless steel webnet provided a large surface area, good ventilation and good utilization of UV light. The TiO_2 films showed a uniform anatase structure with particle sizes about 10 nm. The photocatalytic activity was related to its crystallization and thickness. The thickening crystallization of TiO_2 thin film was evaluated by the photocatalytic oxidation of gaseous formaldehyde in a cylindrical photoreactor. When the film thickness exceeded the certain value (about 250 nm), the activity remained unchanged.

Kim et al., 2001 tried to find the influence of calcination temperature on structural and optical properties of TiO_2 thin films prepared by sol-gel dip coating. The X-ray diffraction (XRD) results showed that TiO_2 thin film calcined at 300 ^{o}C was amorphous, and transform into the anatase phase at 400 ^{o}C and into the rutile phase at 1000 ^{o}C. The crystallization increased with increasing calcination temperature. The refractive index of TiO_2 thin films was increased with the increasing calcination temperature, the film thickness and the porosity of TiO_2 thin films was decreased.

2.3 The sol-gel process

At present, many researchers focus on coated TiO_2 thin films onto carrier surfaces derived from the sol-gel method (Kim and Anderson, 1994). The sol-gel process is a method used to synthesize ceramics and glass of several metal oxides through the hydrolysis and polycondensation (Brinker and Scherer, 1990). A sol is a colloidal suspension of solid particles in a liquid phase. A gel is a substance which encloses an interconnected solid particle within a liquid phase. The reaction that gives a gel is polycondensation or evaporation of the solvent (Brinker and Scherer, 1990). In the sol-gel process, the precursors of colloid maintain a metal or metalloid element surrounded by ligands (Sonawane, 2002). Generally, the transformation processes of the sol-gel technique can be explained as shown below:

(1) Hydrolysis of metal alkoxide;

$$M\text{-}OR + H_2O \longrightarrow M\text{-}OH + R\text{-}OH \qquad (Eq.5)$$

(2) Condensation or evaporation of hydrolyzed molecules to combine oxygen or metaloxane group;

$$M\text{-}OH + R\text{-}OM \longrightarrow M\text{-}O\text{-}M + R\text{-}OH \qquad (Eq.6)$$

$$M\text{-}OH + HO\text{-}M \longrightarrow M\text{-}O\text{-}M + H_2O \qquad (Eq.7)$$

This polymerization could result as huge molecules. In the sol-gel film deposition, evaporation is generally depended upon to solidify the coating. The most important factor

in the rate of evaporation is the rate of diffusion of the vapor away from the film surface (Brinker, 1990).

Regarding to the TiO_2 thin film preparation, the TiO_2 sol solution can be prepared following the upper pathway after the hydrolysis and polycondensation. The TiO_2 sol is formed as a xerogel film before the heat-treatment, and then it would be condensed to become a dense film getting stuck on carriers as shown in Figure 2.4.
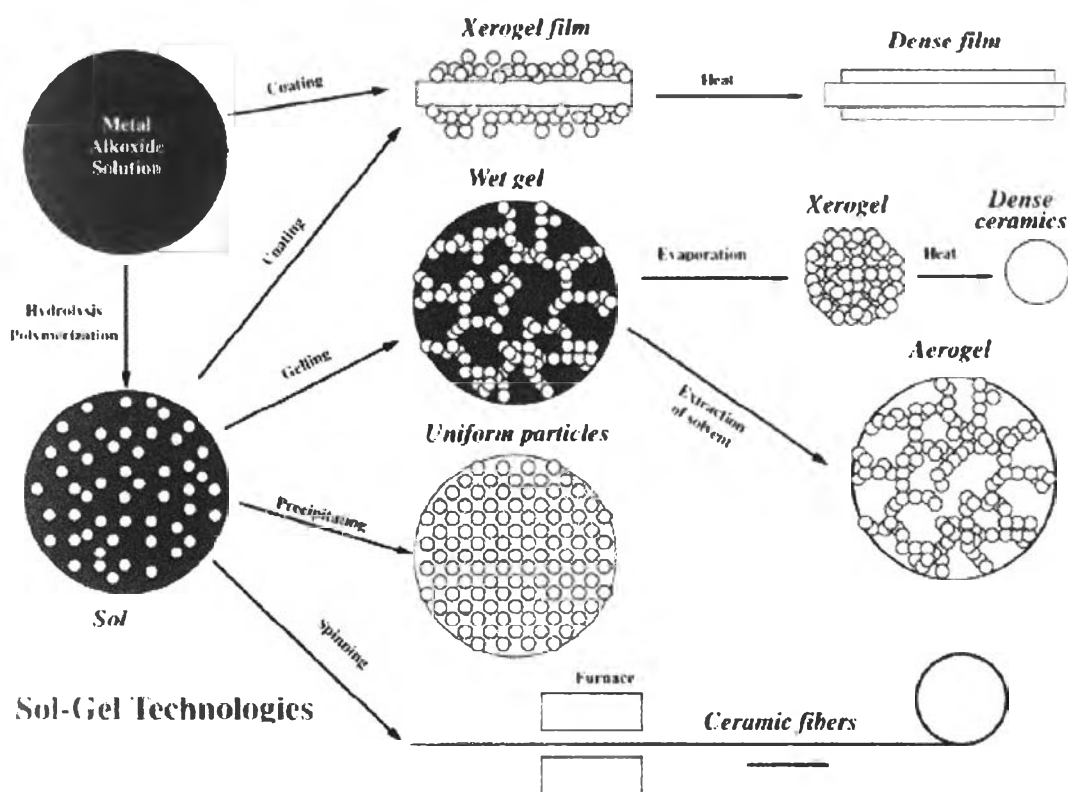

Figure 2.4   the schematic of the sol-gel technologies
(http://www.chemat.com/assets/ images/Flowchat72.jpg: Available: Feb 20, 2006)

The advantages of this technique are its less use of equipment, its cost being less expensive and the ability it has to control the microstructure of the deposited film, e.g. the pore volume, pore size and surface area.

In this research, the film formation was produced by the dip coating technique which could be divided into five stages: (a) immersion, (b) start-up, (c) deposition, (d) drainage and (e) evaporation. The continuous dip coating was simpler because it separated the immersion step from the other stages, which essentially eliminated start-up and hided drainage in the deposited film. Figure 2.5 showed the stages of the dip coating process.
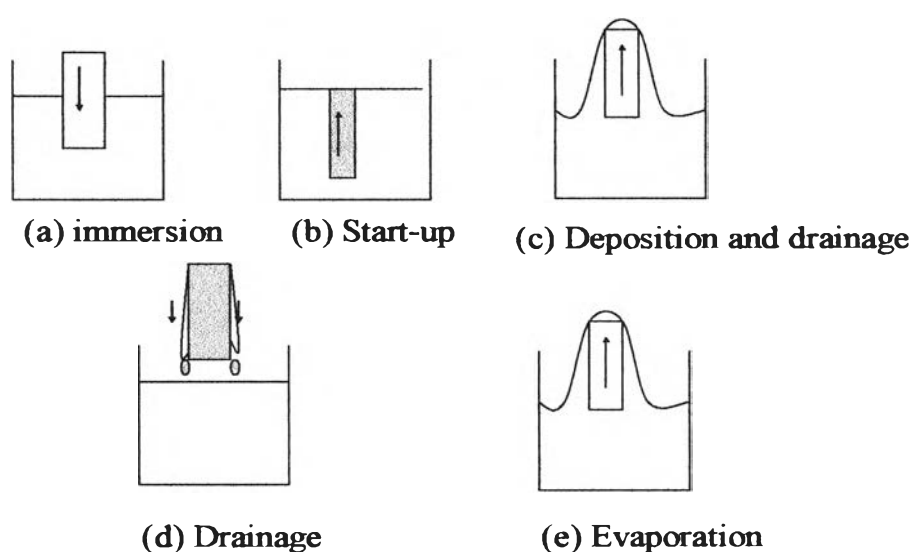

(a) immersion   (b) Start-up   (c) Deposition and drainage

(d) Drainage   (e) Evaporation

Figure 2.5   the stages of the dip coating process

(Brinker and Scherer, 1990)

2.4   Fixed bed photocatalytic reactor (FBPR)

In this work, a fixed bed photocatalytic reactor using TiO_2 as a photocatalyst was studied for the photocatalytic reduction of chromium (VI). TiO_2 was used in its immobilized form using a stainless steel plate as a support.

The first prototype of this reactor was developed at Unicamp by Kondo et al., 1990, later studied by Hilfendorf et al., 1992 and examined by Nogueira and Jardim, 1996. After that, a solar fixed bed reactor overcame any need for separation and received increased interest as a low energy alternative with the recent development of a number of pilot scale reactors (Bahnemann et al., 1999; Zhang et al., 1994; Muradov, 1994; Pugh et al., 1995; Bahnemann et al., 1999).

The advantage of this reactor is that the UV irradiation can react with the catalyst surface area directly. So the degradation of contaminants can increase significantly.

Nogueira and Jardim, 1996 studied TiO_2 fixed bed reactor for water decontamination using solar light. The immobilized TiO_2 was coated on a glass plate. The influence of parameters such as the slope of the plate, solar light intensity, flow rate and molar flow rate were investigated. Dichloroacetic acid (DCA) was used as a model compound. Experiments with recirculation suggested no mass transfer limitations in this system. DCA was mineralized in the production of quantitative amounts of chloride ions. It was showed that a linear dependence of degradation with solar light intensity. The system was currently restricted to low flows.

Feitz et al., 2000 found that two pilot scale fixed bed reactor designs were evaluated by assessing the processing rate for 2 mg/L. The total volume of packed-bed and coated-mesh were 140 and 20 mg m^{-2} h^{-1}, respectively. The improvement in the processing rate was achieved by ensuring a grater available photocatalyst surface area, increasing the contact time, and maintaining turbulent conditions and a sufficient oxygen supply. The packed bed reactor achieved a rapid 99.3 % removal of low levels of phenol under sunny conditions. It was suggested that a fixed bed photocatalytic reactor was highly suitable for the degradation of contaminated water.

Dijkstra et al., 2001 compared three reactors designs for photocatalytic water purification. The photocatalytic degradation of formic acid was different compared to a suspended system, an immobilized system with a coated wall and an immobilized system packed with coated glass beads. In the suspended system and the packed bed reactor

appeared to have the low pseudo-zero-order kinetics, and both these systems had no mass transfer limitations. On the other hand, the tubular reactor with the catalyst coated on the wall did suffer from mass transfer limitation. The performance of the packed bed reactor with high amounts of catalyst present in the reactor was better for the larger glass beads. They suggested the reactor design for an industrial scale could focus on an immobilized system to avoid the post-annealing treatment which was costly.

Chan et al., 2002 used a solar photocatalytic thin film cascade reactor for the treatment of benzoic acid containing in wastewater. The reactor was constructed within stainless steel plates coated with TiO_2 catalyst were arranged in a cascade configuration in the reactor. The percentage removal of TOC in 100 ppm benzoic acid increased from 30% to 83% by adding 30 wt% of hydrogen peroxide solution. The waterfall effect introduced by the cascade design could promote mass transport and aeration in the solution film.

Mehrvar et al., 2002 investigated the preliminary analysis of a tellerette packed-bed photocatalytic reactor in which titanium dioxide was immobilized on stainless steel tellerette packings. The experiments revealed that mass transfer limitations in this packed bed photoreactor were not significant during the photocatalytic degradation of 1,4-dioxane. However, the need with respect to optimizing the tellerette dimensions, bed radius and photocatalytic performance could be investigated. It may have more potential.

Tuprakay and Liengcharernsit, 2005 studied the photoreduction of chromium (VI) using immobilized TiO_2 on polyester resin within a fixed bed batch reactor. High reduction capacity was obtained at 25 ppm as an initial Cr (VI) concentration under 171 W/m^2 light intensity. Adsorption capacity increased with an increasing concentration, and the surface area of immobilized TiO_2 limited the reduction efficiency. The lifetime of TiO_2 was approximately 14 hours. It was not necessary to regenerate TiO_2 for the reduction reaction. Besides, 3 M. NaOH was suggested as an optimum solution for regenerating TiO_2 immobilized on polyester resin. The fresh TiO_2 was more active than regenerated TiO_2, while the regenerated TiO_2 could adsorb chromium more than fresh TiO_2.

2.5 Factors influencing the TiO₂ thin layer characteristics

The characteristics of TiO₂ thin films obtained from the sol-gel method were controlled by the addition of acetyl acetone, the calcination temperature, the number of coating cycles and the appropriate wavelengths. The effects of these parameters were reported as follows:

2.5.1 The addition of acetyl acetone

In the preparation of such TiO₂ thin films with controlled surface structure was the adding of the organic or polymers components into the starting solution under low humidity conditions (Negishi et al., 1995).

Guillard et al., 2002 studied that the adhesion properties of supported TiO₂ thin films prepared by different sol-gel method provided the different photocatalytic activities. The thinkness of TiO₂ thin films loading and the photocatalytic activities were influenced by the nature of the stabilizing agent. In contrast, the organic titanium precursor, as well as the solvent and the absence of stabilizing agents were determined for the resulting photocatalytic activities. Acetyl acetone was used as a kind of stabilizing agent to modify the surface morphology and improve the stability.

Djaoued et al., 2002 reported that acetyl acetone, diethanolamine and polyethylene glycol used as complexing agents were studied the effect of the anatase and rutile phase transition of TiO₂ thin films during the heat-treatment. The starting precursors were titaniumtetraisopropoxide: ethanol: H_2O: complexing agent employed in the preparation of TiO₂ solution. The results showed that the phase transition strongly depended on the complexing agent. Besides, diethanolamine and polyethylene glycol preceded the anatase to rutile trasition from 750 °C to 800 °C, respectively. On the other hand, acetyl acetone could stabilize the anatase phase at 900 °C. The size of nanocrystalline structure of TiO₂ would increase proportionally due to the increasing of temperatures.

2.5.2 The calcination temperatures

Nishide and Mizukami, 1999 found the effect of ligands on crystal structures and optical properties of TiO_2 prepared by sol-gel processes. The TiO_2 prepared with 2- (2-methoxyethoxy) ethanol (MEE) ligand crystallized to anatase at firing temperatures between 350-400 °C. However, the intensity of the anatase peaks increased at 500 °C and 530 °C. XRD patterns of titanium films prepared with MEE and fired at 300 °C and 350 °C showed no peaks in the measured region.

Ahn et al., 2003 investigated that the variation of structural and optical properties of sol-gel TiO_2 thin films with catalyst concentration and calcination temperature. TiO_2 thin films were embedded on quartz glass by the sol-gel process. The TiO_2 thin films were amorphous would transform into the anatase phase at 400-600 °C and into the anatase to rutile phase at 800 °C and further into the rutile phase at 1000 °C. The crystalline size of TiO_2 thin films has been increased with the increasing calcination temperature and catalyst concentration. The transmittance of the deposited TiO_2 thin films calcined at 800-1000 °C were significantly reduced in the wavelength range of 300-800 nm corresponding to the change of crystallite phase and increased particle size. The refractive index of TiO_2 thin films was increased with increasing calcination temperature and catalyst concentration. Meanwhile, the porosity of TiO_2 thin films was decreased.

According to the surface area, porosity, crystal size and the ratio between anatase and rutile were the effect of the changing firing temperature. In summary, the calcination temperaturea were an important parameter influencing the efficiency of photocatalysis (Yoko et al., 1991).

2.5.3 The number of coating cycles

Yoko et al., 1995 reported that photoelectrochemical properties of TiO_2 coating films prepared using different solvents by the sol-gel method. In order to increase the film thickness, the dip coating process was repeated with respect to 5, 7, 10 and 15 times.

It took 10 minutes for heat-treated coating TiO_2 films at 500 °C after each dipping. For 5 time deposited TiO_2 was reheated to further heat-treatment at 500, 600, 700, 800 and 900 °C for various periods of time. In contrast, it is of value to note that a thicker film than required gave a higher voltage drop across it, if the film resistance is high. So, the electrode might have an optimum thickness which ensured the best energy conversion efficiency.

Additionally, the supporting materials for TiO_2 should be good adhesion and bad for degradation the catalyst activity thorough the process. Different types of catalyst carriers, glass plates, fiber optics, quartz, silica bead and stainless steel, were employed (Pozzo et al., 1997).

2.5.4 The appropriate wavelengths

Hermann, 1999 declared that the variation of the reaction rate as a function of the wavelength with a threshold corresponding to its band gap energy. Regard to the band gap energy, it is equal to 3.2 eV which requires $\lambda \leq 400$ nm, i.e., near UV wavelength (UV-A). Moreover, it has to be concerned about the adsorption of reactants.

Some authors have studied that the increase of light intensity results in an increase of photodegradation rate of organic compounds with artificial light. At low intensities, a linear dependence is considered, while at higher intensities this linearity no longer holds and square root dependence is observed (Okamoto et al., 1985; Blake et al., 1991; Ollis, 1991). This situation can be a limitation for the use of concentrated solar systems, when the increase of degradation rate is not followed by the same light concentration.

2.6 Chromium

2.6.1 Properties of chromium

Chromium is a metallic element with oxidation states ranging from chromium (-II) to chromium (+VI). The important valence states of chromium are II, III, and VI. Elemental chromium, chromium (0), does not occur naturally. The divalent state (II or chromous) is relatively unstable and is readily oxidized to the trivalent (III or chromic) state. Chromium compounds are stable in the trivalent state and occur in nature in this state in ores, such as ferrochromite ($FeCr_2O_4$). The hexavalent (VI or chromate) is the second most stable state. However, hexavalent chromium rarely occurs naturally, but is produced from anthropogenic sources (Ku et al., 2001).

2.6.2 Toxicology

Trivalent chromium, Cr (III), is an essential nutrient and is necessary for the metabolism of sugars and for many enzyme reactions. Chromium is a common ingredient in many vitamin and mineral supplements. While, hexavalent chromium, Cr (VI) is a carcinogen because of the carcinogenic properties of some chromium compounds, a risk-based drinking water.

Cr (VI) is known to cause cancer in humans when inhaled. A number of scientific studies have found elevated rates of lung cancer in workers with occupational exposure to Cr (VI) by inhalation. A few studies exposed to Cr (VI) by inhalation have shown an increase in cancers of the gastrointestinal tract. There is substantial evidence from laboratory studies that Cr (VI) can damage DNA and is a mutagen. There continues to be uncertainty in the scientific community whether or not Cr (VI) can cause cancer when ingested at levels found in drinking water (NSC, 1998; ATSDR, 2001).

2.6.3 Chromium removal in photocatalysis

Giménez et al., 1995 studied that photocatalytic reduction of chromium (VI) with titania powders in a continuous flow systems. The kinetics and the effect of catalyst concentration have been analyzed. The results showed that a half-order reaction at pH lower than 4, and a first order reaction for pH above 4. The reduction of titania was deactivated at pH higher than 4, due to the fouling of titania caused by chromium hydroxides.

Schrank et al., 2001 found that simultaneous photocatalytic Cr (VI) reduction and dye oxidation in a TiO_2 slurry reactor. In neutral pH, Cr (VI) is not reduced, because Cr (VI) cannot adsorb on TiO_2 surface. The dye is almost completely degraded by both acidic and neutral pH. The main factors influencing both reactions are the concentration of Cr (VI) and dye and the pH. In the simultaneous reduction-oxidation process, the reduction of Cr (VI) can be quicker than the single process, giving synergism between the oxidation and reduction reactions.

Lin et al., 1993 reported that the thermodynamics aspects of the photocatalytic reduction of Cr (VI) on TiO_2 are contrasted for pH 0 and pH 10. The thermodynamically less favorable in basic media provided the photocorrosion of TiO_2. Dissolved oxygen is shown to inhibit the reduction of Cr (VI). Langmuir model was used to reveal adherence of the initial rate of Cr (VI) reduction via a preliminary kinetics analysis.